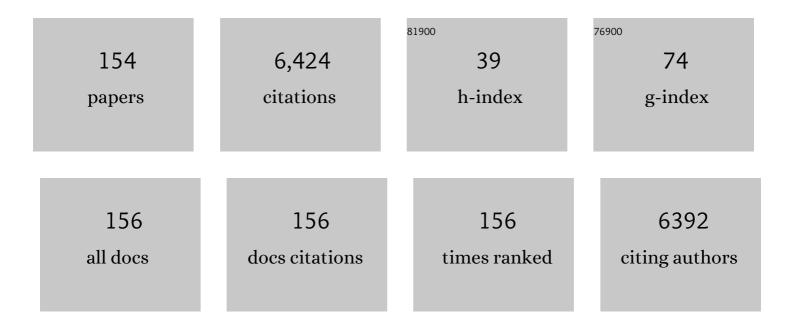
## **Chang Min Park**

List of Publications by Year in descending order

Source: https://exaly.com/author-pdf/8083375/publications.pdf Version: 2024-02-01



#	Article	IF	CITATIONS
1	Percutaneous transthoracic catheter drainage for lung abscess: a systematic review and meta-analysis. European Radiology, 2022, 32, 1184-1194.	4.5	11
2	Value of a deep learning-based algorithm for detecting Lung-RADS category 4 nodules on chest radiographs in a health checkup population: estimation of the sample size for a randomized controlled trial. European Radiology, 2022, 32, 213-222.	4.5	2
3	Deep Learning for Lung Cancer Nodal Staging and Real-World Clinical Practice. Radiology, 2022, 302, 212-213.	7.3	6
4	Definitions of Central Tumors in Radiologically Node-Negative, Early-Stage Lung Cancer for Preoperative Mediastinal Lymph Node Staging. Chest, 2022, 161, 1393-1406.	0.8	5
5	Deep Learning for Detecting Pneumothorax on Chest Radiographs after Needle Biopsy: Clinical Implementation. Radiology, 2022, 303, 433-441.	7.3	23
6	Preoperative percutaneous needle lung biopsy techniques and ipsilateral pleural recurrence in stage I lung cancer. European Radiology, 2022, 32, 2683-2692.	4.5	3
7	Validation for measurements of skeletal muscle areas using low-dose chest computed tomography. Scientific Reports, 2022, 12, 463.	3.3	5
8	Artificial intelligence system for identification of false-negative interpretations in chest radiographs. European Radiology, 2022, 32, 4468-4478.	4.5	8
9	No Prognostic Impact of Staging Brain MRI in Patients with Stage IA Non–Small Cell Lung Cancer. Radiology, 2022, 303, 632-643.	7.3	3
10	Deep Learning Prediction of Survival in Patients with Chronic Obstructive Pulmonary Disease Using Chest Radiographs. Radiology, 2022, 305, 199-208.	7.3	12
11	Deep Learning to Optimize Candidate Selection for Lung Cancer CT Screening: Advancing the 2021 USPSTF Recommendations. Radiology, 2022, 305, 209-218.	7.3	10
12	Self-evolving vision transformer for chest X-ray diagnosis through knowledge distillation. Nature Communications, 2022, 13, .	12.8	18
13	Histopathologic Basis for a Chest CT Deep Learning Survival Prediction Model in Patients with Lung Adenocarcinoma. Radiology, 2022, 305, 441-451.	7.3	10
14	Detection of distant metastases in rectal cancer: contrast-enhanced CT vs whole body MRI. European Radiology, 2021, 31, 104-111.	4.5	2
15	Development and validation of a deep learning algorithm detecting 10 common abnormalities on chest radiographs. European Respiratory Journal, 2021, 57, 2003061.	6.7	58
16	Prediction of visceral pleural invasion in lung cancer on CT: deep learning model achieves a radiologist-level performance with adaptive sensitivity and specificity to clinical needs. European Radiology, 2021, 31, 2866-2876.	4.5	19
17	Deep learning–based automated detection algorithm for active pulmonary tuberculosis on chest radiographs: diagnostic performance in systematic screening of asymptomatic individuals. European Radiology, 2021, 31, 1069-1080.	4.5	29
18	Cone-Beam CT-Guided Percutaneous Transthoracic Needle Lung Biopsy of Juxtaphrenic Lesions: Diagnostic Accuracy and Complications. Korean Journal of Radiology, 2021, 22, 1203.	3.4	7

#	Article	IF	CITATIONS
19	2020 Clinical Practice Guideline for Percutaneous Transthoracic Needle Biopsy of Pulmonary Lesions: A Consensus Statement and Recommendations of the Korean Society of Thoracic Radiology. Korean Journal of Radiology, 2021, 22, 263.	3.4	31
20	Use of Artificial Intelligence-Based Software as Medical Devices for Chest Radiography: A Position Paper from the Korean Society of Thoracic Radiology. Korean Journal of Radiology, 2021, 22, 1743.	3.4	29
21	Usefulness of staging chest-CT in patients with operable breast cancer. PLoS ONE, 2021, 16, e0246563.	2.5	0
22	Pleural recurrence after transthoracic needle lung biopsy in stage I lung cancer: a systematic review and individual patient-level meta-analysis. Thorax, 2021, 76, 582-590.	5.6	17
23	Percutaneous transthoracic needle biopsies in immunocompromised hosts with suspicious pulmonary infection: diagnostic yields and complications. Acta Radiologica, 2021, , 028418512110050.	1.1	0
24	Automatic prediction of left cardiac chamber enlargement from chest radiographs using convolutional neural network. European Radiology, 2021, 31, 8130-8140.	4.5	3
25	Central Tumor Location at Chest CT Is an Adverse Prognostic Factor for Disease-Free Survival of Node-Negative Early-Stage Lung Adenocarcinomas. Radiology, 2021, 299, 438-447.	7.3	18
26	COVID-19 pneumonia on chest X-rays: Performance of a deep learning-based computer-aided detection system. PLoS ONE, 2021, 16, e0252440.	2.5	22
27	Deep Learning for Detection of Pulmonary Metastasis on Chest Radiographs. Radiology, 2021, 301, 455-463.	7.3	19
28	Health insurance coverage for artificial intelligence–based medical technologies: focus on radiology. Journal of the Korean Medical Association, 2021, 64, 648-653.	0.3	1
29	Extended application of a CT-based artificial intelligence prognostication model in patients with primary lung cancer undergoing stereotactic ablative radiotherapy. Radiotherapy and Oncology, 2021, 165, 166-173.	0.6	3
30	Deep learning computer-aided detection system for pneumonia in febrile neutropenia patients: a diagnostic cohort study. BMC Pulmonary Medicine, 2021, 21, 406.	2.0	1
31	Applications of artificial intelligence in the thorax: a narrative review focusing on thoracic radiology. Journal of Thoracic Disease, 2021, 13, 6943-6962.	1.4	10
32	Validation of the Eighth Edition Clinical T Categorization System for Clinical Stage IA, Resected Lung Adenocarcinomas: Prognostic Implications of the Ground-Glass Opacity Component. Journal of Thoracic Oncology, 2020, 15, 580-588.	1.1	25
33	Test-retest reproducibility of a deep learning–based automatic detection algorithm for the chest radiograph. European Radiology, 2020, 30, 2346-2355.	4.5	10
34	Utility of FDG PET/CT for Preoperative Staging of Non–Small Cell Lung Cancers Manifesting as Subsolid Nodules With a Solid Portion of 3 cm or Smaller. American Journal of Roentgenology, 2020, 214, 514-523.	2.2	12
35	Performance of a Deep Learning Algorithm Compared with Radiologic Interpretation for Lung Cancer Detection on Chest Radiographs in a Health Screening Population. Radiology, 2020, 297, 687-696.	7.3	45
36	Patterns of percutaneous transthoracic needle biopsy (PTNB) of the lung and risk of PTNB-related severe pneumothorax: A nationwide population-based study. PLoS ONE, 2020, 15, e0235599.	2.5	3

#	Article	IF	CITATIONS
37	Automated identification of chest radiographs with referable abnormality with deep learning: need for recalibration. European Radiology, 2020, 30, 6902-6912.	4.5	9
38	Chest Tube Drainage Versus Conservative Management as the Initial Treatment of Primary Spontaneous Pneumothorax: A Systematic Review and Meta-Analysis. Journal of Clinical Medicine, 2020, 9, 3456.	2.4	3
39	Preoperative CT-based Deep Learning Model for Predicting Disease-Free Survival in Patients with Lung Adenocarcinomas. Radiology, 2020, 296, 216-224.	7.3	82
40	Differentiation of persistent pulmonary subsolid nodules with a solid component smaller than 6 mm: to be invasive adenocarcinoma or not to be?. Journal of Thoracic Disease, 2020, 12, 1754-1757.	1.4	2
41	Growth and Clinical Impact of 6-mm or Larger Subsolid Nodules after 5 Years of Stability at Chest CT. Radiology, 2020, 295, 448-455.	7.3	27
42	Chest Radiographic and CT Findings of the 2019 Novel Coronavirus Disease (COVID-19): Analysis of Nine Patients Treated in Korea. Korean Journal of Radiology, 2020, 21, 494.	3.4	496
43	Deep learning algorithm for surveillance of pneumothorax after lung biopsy: a multicenter diagnostic cohort study. European Radiology, 2020, 30, 3660-3671.	4.5	32
44	Clinical Validation of a Deep Learning Algorithm for Detection of Pneumonia on Chest Radiographs in Emergency Department Patients with Acute Febrile Respiratory Illness. Journal of Clinical Medicine, 2020, 9, 1981.	2.4	24
45	CT-based deep learning model to differentiate invasive pulmonary adenocarcinomas appearing as subsolid nodules among surgical candidates: comparison of the diagnostic performance with a size-based logistic model and radiologists. European Radiology, 2020, 30, 3295-3305.	4.5	25
46	Extension of Coronavirus Disease 2019 on Chest CT and Implications for Chest Radiographic Interpretation. Radiology: Cardiothoracic Imaging, 2020, 2, e200107.	2.5	59
47	Artificial Intelligence in Health Care: Current Applications and Issues. Journal of Korean Medical Science, 2020, 35, e379.	2.5	46
48	Clinical Implementation of Deep Learning in Thoracic Radiology: Potential Applications and Challenges. Korean Journal of Radiology, 2020, 21, 511.	3.4	48
49	Implementation of a Deep Learning-Based Computer-Aided Detection System for the Interpretation of Chest Radiographs in Patients Suspected for COVID-19. Korean Journal of Radiology, 2020, 21, 1150.	3.4	41
50	Establishment of a Nationwide Korean Imaging Cohort of Coronavirus Disease 2019. Journal of Korean Medical Science, 2020, 35, e413.	2.5	14
51	Undetected Lung Cancer at Posteroanterior Chest Radiography: Potential Role of a Deep Learning–based Detection Algorithm. Radiology: Cardiothoracic Imaging, 2020, 2, e190222.	2.5	14
52	Risk of pleural recurrence after percutaneous transthoracic needle biopsy in stage I non-small-cell lung cancer. European Radiology, 2019, 29, 270-278.	4.5	17
53	CT-defined Visceral Pleural Invasion in T1 Lung Adenocarcinoma: Lack of Relationship to Disease-Free Survival. Radiology, 2019, 292, 741-749.	7.3	29
54	Can Artificial Intelligence Fix the Reproducibility Problem of Radiomics?. Radiology, 2019, 292, 374-375.	7.3	19

#	Article	IF	CITATIONS
55	Deep Learning for Chest Radiograph Diagnosis in the Emergency Department. Radiology, 2019, 293, 573-580.	7.3	107
56	Non-diagnostic Results of Percutaneous Transthoracic Needle Biopsy: A Meta-analysis. Scientific Reports, 2019, 9, 12428.	3.3	10
57	Consolidation-to-tumor ratio and tumor disappearance ratio are not independent prognostic factors for the patients with resected lung adenocarcinomas. Lung Cancer, 2019, 137, 123-128.	2.0	24
58	Evaluation of maximum standardized uptake value at fluorine-18 fluorodeoxyglucose positron emission tomography as a complementary T factor in the eighth edition of lung cancer stage classification. Lung Cancer, 2019, 134, 151-157.	2.0	2
59	Age―and genderâ€specific disease distribution and the diagnostic accuracy of CT for resected anterior mediastinal lesions. Thoracic Cancer, 2019, 10, 1378-1387.	1.9	14
60	Learning Curve of C-Arm Cone-beam Computed Tomography Virtual Navigation-Guided Percutaneous Transthoracic Needle Biopsy. Korean Journal of Radiology, 2019, 20, 844.	3.4	4
61	Clinical T categorization in stage IA lung adenocarcinomas: prognostic implications of CT display window settings for solid portion measurement. European Radiology, 2019, 29, 6069-6079.	4.5	8
62	Serial Texture Analyses on ADC Maps for Evaluation of Antiangiogenic Therapy in Rat Breast Cancer. Anticancer Research, 2019, 39, 1875-1882.	1.1	1
63	Development and Validation of a Deep Learning–Based Automated Detection Algorithm for Major Thoracic Diseases on Chest Radiographs. JAMA Network Open, 2019, 2, e191095.	5.9	284
64	Discrimination of Mental Workload Levels From Multi-Channel fNIRS Using Deep Leaning-Based Approaches. IEEE Access, 2019, 7, 24392-24403.	4.2	43
65	Persistent pulmonary subsolid nodules: How long should they be observed until clinically relevant growth occurs?. Journal of Thoracic Disease, 2019, 11, S1408-S1411.	1.4	3
66	Analysis of Complications of Percutaneous Transthoracic Needle Biopsy Using CT-Guidance Modalities In a Multicenter Cohort of 10568 Biopsies. Korean Journal of Radiology, 2019, 20, 323.	3.4	42
67	Implication of total tumor size on the prognosis of patients with clinical stage IA lung adenocarcinomas appearing as part-solid nodules: Does only the solid portion size matter?. European Radiology, 2019, 29, 1586-1594.	4.5	4
68	Nondiagnostic Percutaneous Transthoracic Needle Biopsy of Lung Lesions: A Multicenter Study of Malignancy Risk. Radiology, 2019, 290, 814-823.	7.3	42
69	Effect of CT Reconstruction Algorithm on the Diagnostic Performance of Radiomics Models: A Task-Based Approach for Pulmonary Subsolid Nodules. American Journal of Roentgenology, 2019, 212, 505-512.	2.2	19
70	Development and Validation of a Deep Learning–based Automatic Detection Algorithm for Active Pulmonary Tuberculosis on Chest Radiographs. Clinical Infectious Diseases, 2019, 69, 739-747.	5.8	150
71	Clinical T Category of Non–Small Cell Lung Cancers: Prognostic Performance of Unidimensional versus Bidimensional Measurements at CT. Radiology, 2019, 290, 807-813.	7.3	12
72	Thoracic recurrence in patients with curatively-resected colorectal cancer: incidence, risk factors, and value of chest CT as a postoperative surveillance tool. European Radiology, 2019, 29, 4303-4314.	4.5	0

#	Article	IF	CITATIONS
73	A simple prediction model using size measures for discrimination of invasive adenocarcinomas among incidental pulmonary subsolid nodules considered for resection. European Radiology, 2019, 29, 1674-1683.	4.5	15
74	Development and Validation of Deep Learning–based Automatic Detection Algorithm for Malignant Pulmonary Nodules on Chest Radiographs. Radiology, 2019, 290, 218-228.	7.3	372
75	Application of Artificial Intelligence in Lung Cancer Screening. Journal of the Korean Society of Radiology, 2019, 80, 872.	0.2	1
76	Diagnostic Accuracy of Percutaneous Transthoracic Needle Lung Biopsies: A Multicenter Study. Korean Journal of Radiology, 2019, 20, 1300.	3.4	42
77	Improving the prediction of lung adenocarcinoma invasive component on CT: Value of a vessel removal algorithm during software segmentation of subsolid nodules. European Journal of Radiology, 2018, 100, 58-65.	2.6	11
78	Cone beam computed tomography virtual navigation-guided transthoracic biopsy of small (≤ cm) pulmonary nodules: impact of nodule visibility during real-time fluoroscopy. British Journal of Radiology, 2018, 91, 20170805.	2.2	9
79	Critical Test Result Notification via MobileÂPhone-Based Automated Text Message System in the Radiologic Field: Single Institutional Experience. Journal of the American College of Radiology, 2018, 15, 973-979.	1.8	4
80	Evaluation of T categories for pure ground-glass nodules with semi-automatic volumetry: is mass a better predictor of invasive part size than other volumetric parameters?. European Radiology, 2018, 28, 4288-4295.	4.5	15
81	Time-dependent analysis of incidence, risk factors and clinical significance of pneumothorax after percutaneous lung biopsy. European Radiology, 2018, 28, 1328-1337.	4.5	38
82	Pulmonary subsolid nodules: value of semi-automatic measurement in diagnostic accuracy, diagnostic reproducibility and nodule classification agreement. European Radiology, 2018, 28, 2124-2133.	4.5	24
83	Risk factors for haemoptysis after percutaneous transthoracic needle biopsies in 4,172 cases: Focusing on the effects of enlarged main pulmonary artery diameter. European Radiology, 2018, 28, 1410-1419.	4.5	19
84	Repeat biopsy of patients with acquired resistance to EGFR TKIs: implications of biopsy-related factors on T790M mutation detection. European Radiology, 2018, 28, 861-868.	4.5	20
85	Current perspectives for the size measurement of screening-detected lung nodules. Journal of Thoracic Disease, 2018, 10, 1242-1244.	1.4	5
86	Pulmonary Subsolid Nodules: An Overview & Management Guidelines. Journal of the Korean Society of Radiology, 2018, 78, 309.	0.2	4
87	Measurement of Multiple Solid Portions in Part-Solid Nodules for T Categorization: Evaluation of Prognostic Implication. Journal of Thoracic Oncology, 2018, 13, 1864-1872.	1.1	14
88	Cone-Beam CT Virtual Navigation-Guided Percutaneous Needle Biopsy of Suspicious Pleural Metastasis: A Pilot Study. Korean Journal of Radiology, 2018, 19, 872.	3.4	4
89	Bronchovascular injury associated with clinically significant hemoptysis after CT-guided core biopsy of the lung: Radiologic and histopathologic analysis. PLoS ONE, 2018, 13, e0204064.	2.5	11
90	Open Bronchus Sign on CT: A Risk Factor for Hemoptysis after Percutaneous Transthoracic Biopsy. Korean Journal of Radiology, 2018, 19, 880.	3.4	7

#	Article	IF	CITATIONS
91	Frequency, outcome, and risk factors of contrast media extravasation in 142,651 intravenous contrast-enhanced CT scans. European Radiology, 2018, 28, 5368-5375.	4.5	18
92	Incidence of Breakthrough Reaction in Patients with Prior Acute Allergic-Like Reactions to Iodinated Contrast Media according to the Administration Route. Korean Journal of Radiology, 2018, 19, 352.	3.4	13
93	Nodule Classification on Low-Dose Unenhanced CT and Standard-Dose Enhanced CT: Inter-Protocol Agreement and Analysis of Interchangeability. Korean Journal of Radiology, 2018, 19, 516.	3.4	4
94	Persistent part-solid nodules with solid part of 5Âmm or smaller: Can the â€~follow-up and surgical resection after interval growth' policy have a negative effect on patient prognosis?. European Radiology, 2017, 27, 195-202.	4.5	18
95	Comparison of the effects of model-based iterative reconstruction and filtered back projection algorithms on software measurements in pulmonary subsolid nodules. European Radiology, 2017, 27, 3266-3274.	4.5	17
96	Non-specific benign pathological results on transthoracic core-needle biopsy: how to differentiate false-negatives?. European Radiology, 2017, 27, 3888-3895.	4.5	33
97	Realâ€ŧime respiratory phase matching between 2D fluoroscopic images and 3D <scp>CT</scp> images for precise percutaneous lung biopsy. Medical Physics, 2017, 44, 5824-5834.	3.0	4
98	Predictive CT Features of Visceral Pleural Invasion by T1-Sized Peripheral Pulmonary Adenocarcinomas Manifesting as Subsolid Nodules. American Journal of Roentgenology, 2017, 209, 561-566.	2.2	38
99	CT assessment-based direct surgical resection of part-solid nodules with solid component larger than 5Âmm without preoperative biopsy: experience at a single tertiary hospital. European Radiology, 2017, 27, 5119-5126.	4.5	19
100	Retrospective assessment of interobserver agreement and accuracy in classifications and measurements in subsolid nodules with solid components less than 8mm: which window setting is better?. European Radiology, 2017, 27, 1369-1376.	4.5	27
101	The prognostic value of CT radiomic features for patients with pulmonary adenocarcinoma treated with EGFR tyrosine kinase inhibitors. PLoS ONE, 2017, 12, e0187500.	2.5	27
102	Percutaneous transthoracic localization of pulmonary nodules under C-arm cone-beam CT virtual navigation guidance. Diagnostic and Interventional Radiology, 2016, 22, 224-230.	1.5	11
103	Evaluation of Semi-automatic Segmentation Methods for Persistent Ground Glass Nodules on Thin-Section CT Scans. Healthcare Informatics Research, 2016, 22, 305.	1.9	14
104	Ossification of the Medial Clavicular Epiphysis on Chest Radiographs: Utility and Diagnostic Accuracy in Identifying Korean Adolescents and Young Adults under the Age of Majority. Journal of Korean Medical Science, 2016, 31, 1538.	2.5	7
105	Measurement Variability of Persistent Pulmonary Subsolid Nodules on Same-Day Repeat CT: What Is the Threshold to Determine True Nodule Growth during Follow-Up?. PLoS ONE, 2016, 11, e0148853.	2.5	19
106	Impact of Reconstruction Algorithms on CT Radiomic Features of Pulmonary Tumors: Analysis of Intra- and Inter-Reader Variability and Inter-Reconstruction Algorithm Variability. PLoS ONE, 2016, 11, e0164924.	2.5	108
107	Microscopic Invasions, Prognoses, and Recurrence Patterns of Stage I Adenocarcinomas Manifesting as Part-Solid Ground-Glass Nodules. Medicine (United States), 2016, 95, e3419.	1.0	5
108	Characteristics of benign solitary pulmonary nodules confirmed by diagnostic videoâ€assisted thoracoscopic surgery. Clinical Respiratory Journal, 2016, 10, 181-188.	1.6	13

#	Article	IF	CITATIONS
109	Temporal Changes of Texture Features Extracted From Pulmonary Nodules on Dynamic Contrast-Enhanced Chest Computed Tomography. Investigative Radiology, 2016, 51, 569-574.	6.2	16
110	Tumor Heterogeneity in Lung Cancer: Assessment with Dynamic Contrast-enhanced MR Imaging. Radiology, 2016, 280, 940-948.	7.3	52
111	Software performance in segmenting ground-glass and solid components of subsolid nodules in pulmonary adenocarcinomas. European Radiology, 2016, 26, 4465-4474.	4.5	42
112	Persistent pulmonary subsolid nodules with solid portions of 5Âmm or smaller: Their natural course and predictors of interval growth. European Radiology, 2016, 26, 1529-1537.	4.5	60
113	The effect of late-phase contrast enhancement on semi-automatic software measurements of CT attenuation and volume of part-solid nodules in lung adenocarcinomas. European Journal of Radiology, 2016, 85, 1174-1180.	2.6	15
114	Prognostic Value of Computed Tomography Texture Features in Non–Small Cell Lung Cancers Treated With Definitive Concomitant Chemoradiotherapy. Investigative Radiology, 2015, 50, 719-725.	6.2	89
115	Persistent Pure Ground-Glass Nodules Larger Than 5 mm. Investigative Radiology, 2015, 50, 798-804.	6.2	66
116	Quantitative Computed Tomography Imaging Biomarkers in the Diagnosis and Management of Lung Cancer. Investigative Radiology, 2015, 50, 571-583.	6.2	41
117	Digital Tomosynthesis for Evaluating Metastatic Lung Nodules: Nodule Visibility, Learning Curves, and Reading Times. Korean Journal of Radiology, 2015, 16, 430.	3.4	11
118	Pulmonary Nodule Detection in Patients with a Primary Malignancy Using Hybrid PET/MRI: Is There Value in Adding Contrast-Enhanced MR Imaging?. PLoS ONE, 2015, 10, e0129660.	2.5	13
119	Collateral Ventilation Quantification Using Xenon-Enhanced Dynamic Dual-Energy CT: Differences between Canine and Swine Models of Bronchial Occlusion. Korean Journal of Radiology, 2015, 16, 648.	3.4	3
120	Pulmonary adenocarcinomas appearing as part-solid ground-glass nodules: Is measuring solid component size a better prognostic indicator?. European Radiology, 2015, 25, 558-567.	4.5	75
121	Rapid needle-out patient-rollover approach after cone beam CT-guided lung biopsy: effect on pneumothorax rate in 1,191 consecutive patients. European Radiology, 2015, 25, 1845-1853.	4.5	62
122	PET/MR Imaging for Chest Diseases. Magnetic Resonance Imaging Clinics of North America, 2015, 23, 245-259.	1.1	8
123	C-Arm Cone-Beam CT Virtual Navigation-Guided Percutaneous Mediastinal Mass Biopsy: Diagnostic Accuracy and Complications. European Radiology, 2015, 25, 3508-3517.	4.5	16
124	Transient subsolid nodules in patients with extrapulmonary malignancies: their frequency and differential features. Acta Radiologica, 2015, 56, 428-437.	1.1	14
125	Value of Computerized 3D Shape Analysis in Differentiating Encapsulated from Invasive Thymomas. PLoS ONE, 2015, 10, e0126175.	2.5	11
126	Pulmonary subsolid nodules: what radiologists need to know about the imaging features and management strategy. Diagnostic and Interventional Radiology, 2014, 20, 47-57.	1.5	47

#	Article	IF	CITATIONS
127	C-Arm Cone-Beam CT-guided Percutaneous Transthoracic Needle Biopsy of Lung Nodules: Clinical Experience in 1108 Patients. Radiology, 2014, 271, 291-300.	7.3	163
128	Correlation between the Size of the Solid Component on Thin-Section CT and the Invasive Component on Pathology in Small Lung Adenocarcinomas Manifesting as Ground-Glass Nodules. Journal of Thoracic Oncology, 2014, 9, 74-82.	1.1	190
129	Influence of radiation dose and iterative reconstruction algorithms for measurement accuracy and reproducibility of pulmonary nodule volumetry: A phantom study. European Journal of Radiology, 2014, 83, 848-857.	2.6	46
130	Persistent pulmonary subsolid nodules: model-based iterative reconstruction for nodule classification and measurement variability on low-dose CT. European Radiology, 2014, 24, 2700-2708.	4.5	10
131	Computerized Texture Analysis of Persistent Part-Solid Ground-Glass Nodules: Differentiation of Preinvasive Lesions from Invasive Pulmonary Adenocarcinomas. Radiology, 2014, 273, 285-293.	7.3	203
132	Volume and Mass Doubling Times of Persistent Pulmonary Subsolid Nodules Detected in Patients without Known Malignancy. Radiology, 2014, 273, 276-284.	7.3	105
133	Usefulness of Texture Analysis in Differentiating Transient from Persistent Part-solid Nodules(PSNs): A Retrospective Study. PLoS ONE, 2014, 9, e85167.	2.5	40
134	Percutaneous transthoracic needle biopsy of small (â‰≇Âcm) lung nodules under C-arm cone-beam CT virtual navigation guidance. European Radiology, 2013, 23, 712-719.	4.5	94
135	Pure and Part-Solid Pulmonary Ground-Glass Nodules: Measurement Variability of Volume and Mass in Nodules with a Solid Portion Less than or Equal to 5 mm. Radiology, 2013, 269, 585-593.	7.3	59
136	Does Antiplatelet Therapy Increase the Risk of Hemoptysis During Percutaneous Transthoracic Needle Biopsy of a Pulmonary Lesion?. American Journal of Roentgenology, 2013, 200, 1014-1019.	2.2	26
137	Invasive Pulmonary Adenocarcinomas versus Preinvasive Lesions Appearing as Ground-Glass Nodules: Differentiation by Using CT Features. Radiology, 2013, 268, 265-273.	7.3	260
138	Follicular dendritic cell sarcoma of the mediastinum: CT and <sup>18</sup> Fâ€fluoroâ€2â€deoxyglucose PET findings. Thoracic Cancer, 2013, 4, 203-206.	1.9	7
139	IASLC/ATS/ERS International Multidisciplinary Classification of Lung Adenocarcinoma. Journal of Thoracic Imaging, 2012, 27, 340-353.	1.5	69
140	C-Arm Cone-Beam CT–Guided Percutaneous Transthoracic Needle Biopsy of Small (≤20mm) Lung Nodules: Diagnostic Accuracy and Complications in 161 Patients. American Journal of Roentgenology, 2012, 199, W322-W330.	2.2	94
141	The Effect of Visceral Fat Mass on Pancreatic Fistula after Pancreaticoduodenectomy. Journal of Investigative Surgery, 2012, 25, 169-173.	1.3	38
142	Quantitative analysis of applied force on biopsy needle insertions. Biomedical Engineering Letters, 2012, 2, 249-254.	4.1	2
143	CT-Guided Percutaneous Transthoracic Localization of Pulmonary Nodules Prior to Video-Assisted Thoracoscopic Surgery Using Barium Suspension. Korean Journal of Radiology, 2012, 13, 694.	3.4	59
144	Computer-Aided Detection of Malignant Lung Nodules on Chest Radiographs: Effect on Observers' Performance. Korean Journal of Radiology, 2012, 13, 564.	3.4	27

#	Article	IF	CITATIONS
145	Korean Society of Thoracic Radiology Guideline for Lung Cancer Screening with Low-Dose CT. Journal of the Korean Society of Radiology, 2012, 67, 349.	0.2	9
146	Ground-Glass Nodules on Chest CT as Imaging Biomarkers in the Management of Lung Adenocarcinoma. American Journal of Roentgenology, 2011, 196, 533-543.	2.2	103
147	Initial experience of percutaneous transthoracic needle biopsy of lung nodules using C-arm cone-beam CT systems. European Radiology, 2010, 20, 2108-2115.	4.5	75
148	Transient Part-Solid Nodules Detected at Screening Thin-Section CT for Lung Cancer: Comparison with Persistent Part-Solid Nodules <sup></sup> . Radiology, 2010, 255, 242-251.	7.3	121
149	"Popcorn―Calcifications in a Pulmonary Chondroid Hamartoma. New England Journal of Medicine, 2009, 360, e17.	27.0	9
150	Predictive CT findings of malignancy in ground-glass nodules on thin-section chest CT: the effects on radiologist performance. European Radiology, 2009, 19, 552-560.	4.5	121
151	Dynamic Tumor Staging. New England Journal of Medicine, 2008, 359, e4.	27.0	0
152	Radiation Dose Modulation Techniques in the Multidetector CT Era: From Basics to Practice. Radiographics, 2008, 28, 1451-1459.	3.3	279
153	Pulmonary Nodular Ground-Glass Opacities in Patients With Extrapulmonary Cancers. Chest, 2008, 133, 1402-1409.	0.8	69
154	Nodular Ground-Glass Opacity at Thin-Section CT: Histologic Correlation and Evaluation of Change at Follow-up. Radiographics, 2007, 27, 391-408.	3.3	258